Air Distribution in Rooms, (ROOMVENT 2000)
Editor: H.B. Awbi

13324

EFFECT OF SASH HEIGHT AND OPERATOR ON AIRFLOW IN A FUME HOOD

Allan T. Kirkpatrick and Robert Reither

Department of Mechanical Engineering, Colorado State University,
Fort Collins, CO 80523 USA

ABSTRACT

A three dimensional computational fluid dynamics (CFD) analysis has been used to predict airflow patterns in laboratory fume hoods. The simulation includes bypass fume hood primary operational features including the top and bottom bypasses, front airfoils, and rear slotted baffles. The study included the effects on the fume hood airflow of sash height changes, an operator positioned outside the fume hood, and equipment within the main fume hood chamber. It was shown for conditions of a fully open sash height, a person in front of the fume hood, and an object inside the fume hood, the fume hood experiences a loss of containment of the flow.

KEYWORDS

Fume hoods, airflow modeling, containment, sash effect

INTRODUCTION

The laboratory fume hood is a safety device used in chemical, research, and teaching laboratories. It provides a location at which to work on toxic substances with reduced risk to users. The primary function of the hood is to prevent contaminants from entering the laboratory. The fume hood basically provides an exhausted enclosure, operating at a negative pressure relative to the room, which is intended to vent contaminants away from the user and the laboratory space. There are several types of fume hoods including constant volume or bypass, restricted bypass, and auxiliary air fume hoods.

The subject of this paper is the effect of the fume hood sash position and the presence of the operator in front of the hood on the airflow patterns in a bypass fume hood. The model in the study simulates a bypass type bench fume hood with a vertical sash, as shown schematically in Figure 1. Major features of the bypass type fume hood are a top mounted exhaust duct, top bypass supply, bottom bypass supply, variable height vertical sash, back baffles, and front airfoils. Air enters the main fume hood chamber through one of three locations: sash opening, top bypass, and the bottom bypass formed by the bottom airfoil. The purpose of the top bypass is to maintain a constant volume of air entering the fume hood, regardless of the sash height. The back baffles are positioned such that air is exhausted

directly from the work surface as well as the top of the main fume hood chamber. The front airfoils reduce the amount of turbulence and eddy motion entering the fume hood. In addition, the bottom airfoil is extended beyond the vertical plain of the sash to provide a direct flow (also called floor sweep) across the bottom of the fume hood main chamber.

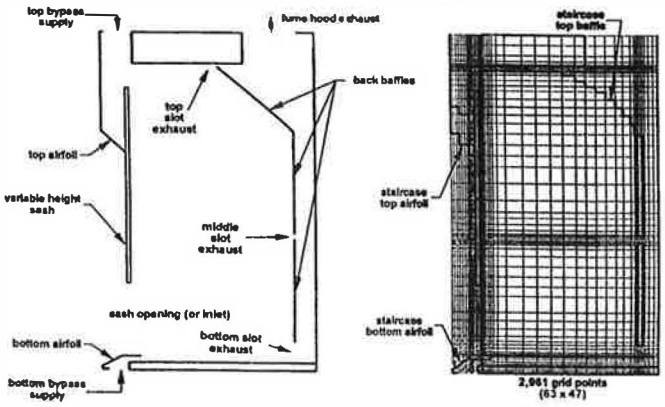

Figure 1: Bypass-type fume hood features

At present fume hoods are designed empirically and tested experimentally. For example, Chang (1994) measured the airflow around an operator standing in front of a fume hood. At present only a small number of fume hood studies have been numerical. Durst and Pereira (1991) performed a numerical analysis of an empty two-dimensional fume hood model, which included a back baffle, to study containment capabilities of fume hoods at selected sash openings. Inclusion of the airfoils, bypasses, and angled slotted baffles in this study furthers the previous numerical studies performed on fume hoods.

COMPUTATIONAL MODEL

A turbulent finite difference model was used for the simulation (Kurabuchi, T., J.B. Fang, and R.A. Grot. 1989). The computational model uses a standard two-equation κ–ε model with buoyancy terms included. The κ–ε model was selected because it is relatively stable and computationally efficient compared with the more complicated Reynolds stress models and is applicable to a wide range of turbulent flows (Neilsen, Peter V., 1998). There are seven non-dimensional equations used by the model: two vector partial differential equations (continuity, momentum), two scalar differential equations (turbulence kinetic energy, dissipation rate of turbulence energy), and one algebraic relationship for turbulent viscosity. There are also seven required empirical constants determined from correlations of experimental data (Launder, B.E., and Spalding, D.B. 1974).

To solve the system of non-linear partial differential equations, the code uses an explicit time marching algorithm, pressure relaxation method, and a central or upwind differencing scheme (Kurabuchi et al. 1989). A marker and cell method is used for the staggered grid. Velocity components are defined at the center of their normal cell faces and the scalar variables (pressure, temperature, turbulence kinetic energy, and dissipation rate of turbulence energy) are defined at the center of the cell. The wall boundary condition for the momentum boundary layer used by the code is based upon the power law

assumption of the velocity profile. A detailed description of these boundary conditions can be found in Knapmiller and Kirkpatrick (1994). A contaminant dispersion study was also performed, using a turbulent contamination diffusion model (Kurabuchi et al. 1989). The converged flow field output file from the flow field calculation is used as input for computing the contaminant dispersion, since the velocity field is independent of the concentration field.

3D COMPUTATIONAL GEOMETRY

The airflow in a fume hood is three dimensional due to the finite width of the main chamber, the airfoils, and the presence of a person and object in front of and inside the fume hood, respectively. The three dimensional computational grid used to model the room and the laboratory fume hood is shown in Figure 2. The model has a room containing the fume hood resting on a cabinet, a person standing on the floor in front of the fume hood, and an object inside the fume hood. In addition, the model contains a variable height sash, top, bottom, and side airfoils, top, middle, and bottom baffles, and a rectangular exhaust. The room is approximately 109.5 inches (2.78 m) high, a half width of the fume hood wide (36", 0.91 m), and three fume hood interior depths long (83.5", 2.12 m). Two sash heights were studied, a nominal working height of 18" (46 cm) and a fully open position at 30.25" (77 cm). The three slot exhaust heights were fixed for all computations at: 0.75" (1.9 cm) top, 1.0" (2.5 cm) middle, and 3.375" (8.6 cm) bottom. Three fume hood depths were selected for the room length because beyond 2.5 fume hood depths the room airflow streamlines are unchanged.

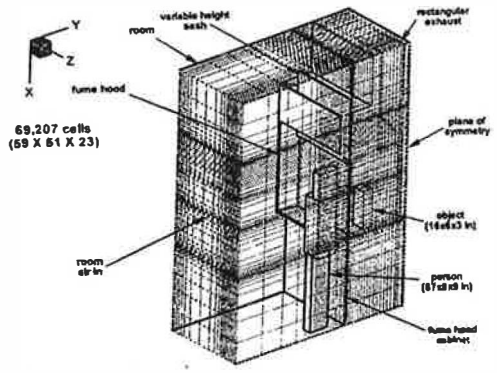

Figure 2: 3D room and fume hood computational grid

As seen in Figure 2 the room, fume hood, person, and object are split down the center in the computational model to take advantage of symmetry. Boundary conditions to start the simulation are as follows: air flows into the room, on the x-z plane at the front of the room, as a uniform flow. This room inlet air is given an initial y-velocity, turbulence energy, and a turbulence dissipation rate. The non-dimensional turbulence energy of the room inlet air is 0.005 and the non-dimensional turbulence dissipation rate is 0.00125; both values are typical of room air motion computations (Kurabuchi et al. 1989). The non-dimensional turbulence energy corresponds to a turbulent intensity of 5.8 percent. The room exhaust is through the rectangular exhaust at the top of fume hood, where only the pressure is specified and the velocity is computed by the model. Power law wall boundary conditions are specified on the ceiling and floor of the room as well as on the back surface of the fume hood. All other surfaces, including those of the fume hood, the person, and the object, have a zero normal velocity boundary condition with no shear. The top of the object in the fume hood releases contaminates, with a non-dimensional boundary value of 1.0.

Grid development of a fume hood model proved to be a very challenging problem. The actual fume hood contains three very thin airfoils, all at different angles, as well as a very thin top baffle at yet another angle. All these angled surfaces are modeled as staircases with an infinitely thin surface between adjacent cells, which have zero normal velocity. There are also three different sized flow entrances each in having their own direction and four exhausts of different sizes in two different directions. The grid contains 69,207 non-uniform cells (59 – x direction, 51 – y direction, 23 – z direction) optimized by size, location, and number of cells to include all of the above features, as well as the person, object, and variable height sash in the same grid. A grid sensitivity study was performed on a two-dimensional model of the room and fume hood. To validate the computations at each sash height, a smoke test and mass balance were performed on an empty fume hood. Further information about the validation experiments is given in Kirkpatrick and Reither (1998). The nominal computation time was 22 hours on a 200 MHz Pentium II desktop PC.

RESULTS

The results for the case of the working sash height set at 18" (46 cm) are shown in Figure 3. Figure 3 and subsequent similar figures show a vertical plane cut at the plane of symmetry of the model. As can be seen in the Figure, the flow enters the room from the left and enters the fume hood at any of the three entrances; sash opening, top bypass, or bottom bypass. The flow then exits the main fume hood chamber through the top, middle, or bottom slot exhausts. As shown in Figure 3 a vortex appears downstream of the sash, and the operator's body generates a small clockwise vortex downstream of the person at approximately waist level. Details of this small vortex are shown in Section A of Figure 3. The vortex is generated by the flow over the top of the person and down their body and the flow coming up between the person's legs. As shown in Figure 4, the computation also predicts that containment is maintained by the fume hood, i.e., there is no reverse flow out of the fume hood entrance, when the sash height is maintained at the nominal 18 (46 cm) working height.

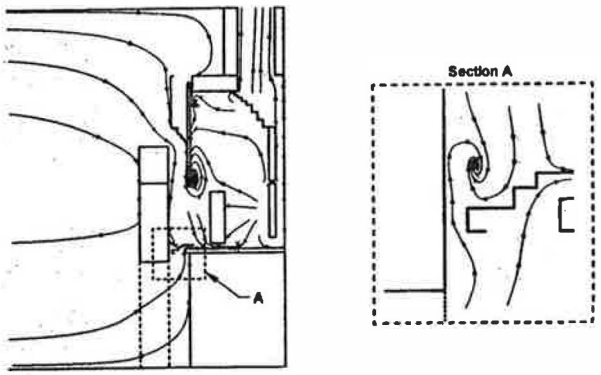

Figure 3: Vertical slice of airflow pattern with sash at nominal 18" (46 cm) sash opening

The airflow for the fully open sash is shown in Figure 5. Similar flow structures (vortices behind the sash and person and recirculation behind the object) are predicted as in the 18" (46 cm) sash height case. Figure 4 shows flow moving from the front of the object inside the fume hood to the small vortex downstream of the person outside of the main fume hood chamber.

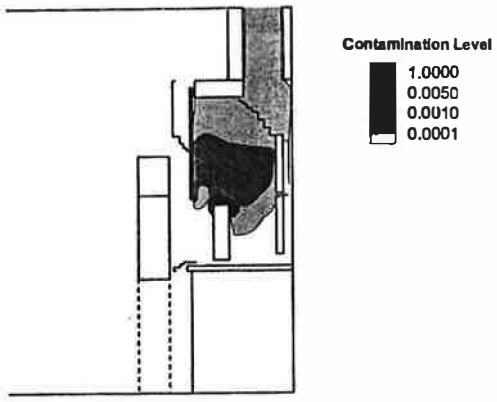

Figure 4: Vertical slice of contamination profiles with sash at nominal 18" (46 cm) sash opening

The flow behind (downstream of) the object in the 30.25" (0.77 m) is predicted to flow over the top of the object and down, with just a slight sweep away from the back baffle. With the sash all the way up, more flow is allowed to pass over the top of the object and less flow is forced around the sides, as seen before in the 18" (0.46 m) sash height case. Section A of Figure 5 shows a small clockwise vortex behind (downstream of) the person of the same size as before, but located a little higher above the waist. Vortices are also seen in a horizontal slice for this configuration. A strong vortex now appears just downstream of the person and a weak flow recirculation exists just downstream of the object. For the fully open sash height, flow is no longer forced down the body of the person by the sash, consequently the flow around the sides of the person generates a vortex. The lowest pressures in the flow field are just downstream of the operator.

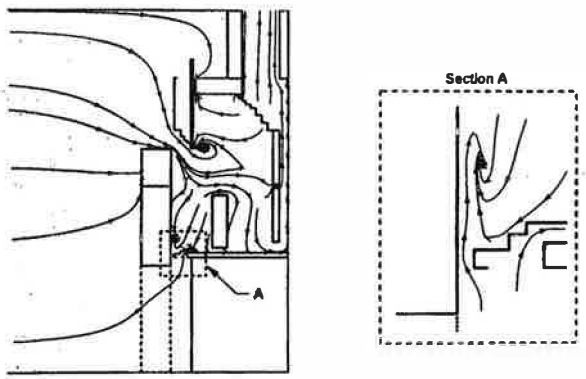

Figure 5: Vertical slice of airflow pattern for fully open sash at 30" (77cm)

Figure 6 displays the results of the contamination computation for the fully open sash. The most significant result for the fully open sash case is the prediction of loss of containment in the main fume hood chamber. This is a consequence of the low pressure vortex structure in front of the operator. As seen in Figure 6, the contaminant follows the airflow patterns of Figure 5. A small concentration of contaminant moves from the top of the object, down the front face of the object, and out of the fume hood main chamber, and into the laboratory space. This represents a failure mode of the fume hood, so that operation of the fume hood with the sash at a fully open height should be avoided.

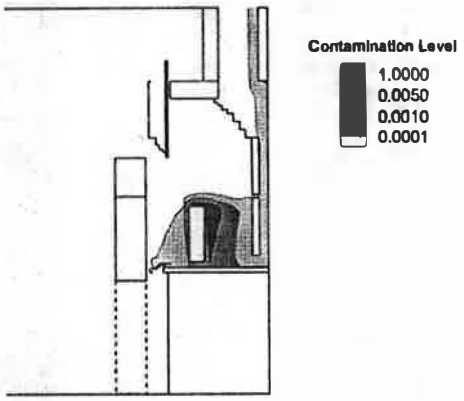

Figure 6: Vertical slice of contamination profiles for fully open sash at 30" (77cm)

SUMMARY AND CONCLUSIONS

The numerical study included the effects on the fume hood airflow of sash height changes, an operator positioned outside the fume hood, and equipment within the main fume hood chamber. With the fume hood sash at a nominal working height, there was no loss of contamination from the hood. However, with a fully open sash in a by-pass fume hood , the presence of a person in front of the fume hood will cause a loss of containment of the flow in the fume hood.

REFERENCES

Chang, S. (1994). Air Velocity Profiles Around a Person Standing in Front of Exhaust Hoods. *ASHRAE Transactions*, **100:2**, 439-447.

Durst, F. and Pereira, J. (1991). Experimental and Numerical Investigations of the Performance of Fume Cupboards. *Building and Environment*. **26:2**, 153-164.

Kirkpatrick A. and Reither R. (1998), Numerical Simulation of Laboratory Fume Hood Airflow Performance, *ASHRAE Transactions*, **104:2.**

Knapmiller, K. and Kirkpatrick A. (1994). Computational Determination of the Behavior of a Cold Air Ceiling Jet in a Room With a Plume. *ASHRAE Transactions*. **100:1**, 677-684.

Kurabuchi, T., Fang J., and Grot R. (1989). A Numerical Method for Calculation of Indoor Airflows Using a Turbulence Model. NISTIR 89-4211. Gaithersburg, MD: National Institute of Standards and Technology.

Launder, B. and Spalding, D. (1974). The Numerical Computation of Turbulent Flows. *Computer Methods in Applied Mechanics and Engineering*. **3**, 269-289.

Neilsen, P. (1998). The Selection of Turbulence Models for the Prediction of Room Airflow. *ASHRAE Transactions*. **104:1**.